

Negative differential resistance in n-type noncompensated silicon at low temperature

A. L. Danilyuk, A. G. Trafimenko, A. K. Fedotov, I. A. Svito, and S. L. Prischepa

Citation: *Applied Physics Letters* **109**, 222104 (2016); doi: 10.1063/1.4968825

View online: <http://dx.doi.org/10.1063/1.4968825>

View Table of Contents: <http://scitation.aip.org/content/aip/journal/apl/109/22?ver=pdfcov>

Published by the [AIP Publishing](#)

Articles you may be interested in

[Ge quantum dot tunneling diode with room temperature negative differential resistance](#)

Appl. Phys. Lett. **97**, 012101 (2010); 10.1063/1.3462069

[Single donor induced negative differential resistance in silicon n-type nanowire metal-oxide-semiconductor transistors](#)

J. Appl. Phys. **107**, 093703 (2010); 10.1063/1.3399999

[Temperature dependence of voltage-controlled negative resistance and electroluminescence in Al – Al₂O₃ – Au diodes](#)

J. Appl. Phys. **104**, 103704 (2008); 10.1063/1.3021092

[High negative differential resistance in silicon quantum dot metal-insulator-semiconductor structure](#)

Appl. Phys. Lett. **89**, 153117 (2006); 10.1063/1.2360888

[Effect of low-temperature annealing on the luminescent lifetime and negative differential resistance of silicon-implanted borosilicate glass](#)

J. Appl. Phys. **94**, 7542 (2003); 10.1063/1.1630366



NEW Special Topic Sections

NOW ONLINE
Lithium Niobate Properties and Applications:
Reviews of Emerging Trends

AIP | Applied Physics
Reviews

Negative differential resistance in n-type noncompensated silicon at low temperature

A. L. Danilyuk,¹ A. G. Trafimenko,¹ A. K. Fedotov,² I. A. Svito,² and S. L. Prischepa¹

¹Belarusian State University of Informatics and Radioelectronics, P. Browka 6, Minsk 220013, Belarus

²Belarusian State University, Nezalezhnastsi Av. 4, Minsk 220030, Belarus

(Received 1 September 2016; accepted 14 November 2016; published online 29 November 2016)

We present the results on low temperature current-voltage characteristics of noncompensated Si doped by Sb. In the temperature range 1.9–2.25 K and at electrical fields smaller than 1 V/cm, the negative differential resistance (NDR) was observed. The external magnetic field enhances the region of the NDR. We attribute this effect to the delocalization of the D^- states in the upper Hubbard band due to the accumulation of the charge injected by current. *Published by AIP Publishing.*

[<http://dx.doi.org/10.1063/1.4968825>]

Interest in the studies on the effect of a negative differential resistance (NDR) in various materials and structures does not subside currently. This is primarily due to the importance of the NDR effect in developing the elements of solid-state electronics, like generators, switches, sensors, memory, etc. These studies are characterized by a very wide range of materials and structures, including graphene,¹ topological insulators,² structures of molecular electronics,³ and semiconductor nano- and heterostructures.^{4–6} Physical mechanisms, determining the NDR, are very diverse. Thus, if the known effects of NDR in bulk semiconductors are mainly associated with the heating of the charge carriers and the emergence of various kinds of instabilities like drift, concentration, etc.⁴ in the nano- and heterostructures, except the field mechanisms, mechanisms associated with a discrete spectrum also appear.⁷ A common feature of the NDR effect in semiconductor materials and structures based on them is its dependence on the physical properties and processes in semiconductors. This imposes certain requirements for their production technology and makes it difficult to fabricate identical devices and their further applications. In particular, mechanisms of the NDR, related to the heating of the electron gas, are characterized by increased noises and power consumption, premature degradation and thermal losses. Structures exhibiting NDR, in which there is no heating of the charge carriers, are often poorly compatible with the silicon technology. The latter is especially important for the formation of various functional elements on a single chip. Therefore, search for the NDR effect in silicon and silicon based structures, which are not related to the heating of the charge carriers, should be regarded as highly relevant.

This paper presents the results of the study of current-voltage characteristics (CVC) of noncompensated common-place commercial n-type silicon with a Sb dopant density $N_d = (1.0 \pm 0.1) \times 10^{18} \text{ cm}^{-3}$ (Ref. 8) (insulating side of the metal-insulator transition—MIT⁹) in the temperature range $T = 1.9\text{--}12 \text{ K}$ and magnetic field H up to 80 kOe. Resistivity at room temperature was $\rho = (0.010 \pm 0.001) \Omega \text{ cm}$. The samples of rectangular shape with dimensions $10 \text{ mm} \times 2 \text{ mm} \times 0.5 \text{ mm}$ were covered by 4 In contacts as electric probes using ultrasonic soldering. The distance between the current (I) (voltage (V)) pads was equal to 8 mm ($l = 3 \text{ mm}$). A dc

current was used to bias the samples. The magnetic field was applied parallel to the sample surface and perpendicular to the direction of the current. Samples were inserted into the cryogenic free measuring system (Cryogenic Ltd., London) with the superconducting solenoid.

For these bulk samples, CVC exhibit unusual behavior in the T range 1.9–2.25 K, appearance of the pronounced NDR region at very low value of the electric field E , not exceeding $E = 1 \text{ V/cm}$. As the temperature increases, CVC are transformed into a linear dependence. In this work, we plot measured CVC as a dependence of the current density J on the average magnitude of the electric field $E = V/l$, $J(E)$.

Fig. 1 shows a series of $J(E)$ curves in zero magnetic field for T range 1.9–3.0 K (Fig. 1(a)) and 3.1–12 K (Fig. 1(b)). All the characteristics were registered for both increasing and decreasing current. The lack of hysteresis indicates the absence of thermal overheating of the sample. The NDR region is observed in the narrow T range 1.9–2.25 K. With increasing temperature, starting from $T = 2.5 \text{ K}$, a gradual transition from nonlinear to linear characteristics occurs (Fig. 1(b)). In Fig. 2(a), we present the $J(E)$ characteristics at $T = 2 \text{ K}$ for magnetic field values from 0 to 80 kOe. It follows that the magnetic field enhances the manifestation of a region with the NDR. In addition, the magnetoresistance (MR) is positive. The temperature increase in the presence of a magnetic field leads to the disappearance of the NDR, as in the absence of a magnetic field. In Fig. 2(b), we show the variation of the $J(E)$ shape with the growth of temperature at $H = 80 \text{ kOe}$. In the inset to Fig. 2(b), the MR versus T is plotted. The MR values were obtained from the initial linear parts of the $J(E)$ curves.

Typical threshold current density for the formation of the NDR region in $J(E)$ characteristics does not exceed 50 mA/cm^2 , and typical threshold electric field E_{th} values are less than 1 V/cm. Such extremely low E_{th} cannot lead to the electrical breakdown. Moreover, the smallness of the electric field can exclude any other field effects, such as Poole-Frenkel, impact ionization, avalanche multiplication or thermionic.

Previous analysis revealed that the transport in the studied samples in the T range 5–25 K is determined by the Mott mechanism ($\ln \rho(T) \sim T^{-1/4}$).⁸ Here, we obtain that in

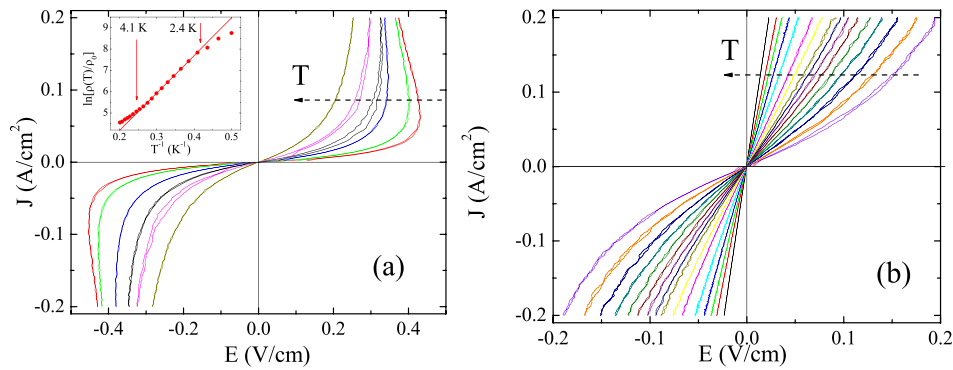


FIG. 1. (a) $J(E)$ curves at different T . From right to left: 1.9, 2.0, 2.25, 2.5, 2.75, and 3.0 K. The arrow indicates the growth direction of the temperature. Inset: $\ln \rho$ versus T^{-1} . Solid line is the result of the best linear fit in these coordinates. Arrows indicate the T range in which simple activation dependence is observed. (b) $J(E)$ curves at different T . From right to left: 3.1, 3.25, 3.5, 3.75, 4.0, 4.25, 4.5, 4.75, 5.0, 5.5, 6.0, 7.0, 8.0, 9.0, 10.0, and 12.0 K. The arrow indicates the growth direction of the temperature. All data are for $H = 0$.

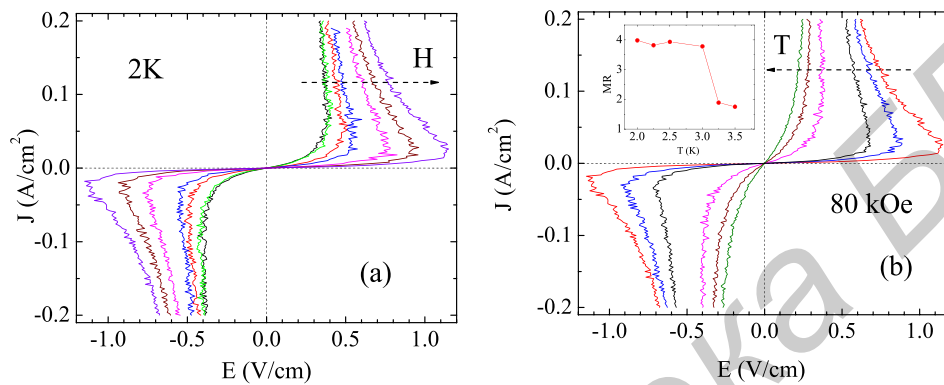


FIG. 2. (a) $J(E)$ curves at $T = 2$ K and different $H = 0, 10, 30, 40, 60, 70,$ and 80 kOe. The arrow indicates the growth direction of the magnetic field. (b) $J(E)$ curves at $H = 80$ kOe and different $T = 2.0, 2.25, 2.5, 3.0, 3.25,$ and 3.5 K. The arrow indicates the growth direction of the temperature. Inset: Magnetoresistance versus temperature at $H = 80$ kOe.

the T range 2–4 K the simple activation mechanism ($\ln \rho(T) \sim T^{-1}$) prevails (see inset to Fig. 1(a)). The activation energy can be estimated as $\epsilon = 1.48 \text{ meV} \approx 17 \text{ K}$ (slope of the solid line in the inset to Fig. 1(a)). Such low ϵ value suggests that two impurity bands apparently participate in conductivity in the T range 2–4 K, upper and lower Hubbard bands.¹⁰

As it was already pointed out, the measured $J(E)$ characteristics with decreasing temperature are transformed from linear Ohmic to the essentially nonlinear dependence. Moreover, for the temperatures, at which the NDR is not

observed, but a strong nonlinearity is present, the small initial linear part of the $J(E)$ characteristic is changed with increasing electric field first to the Child-Langmuir ($J(E) \sim E^{3/2}$) and then to the Mott-Gurney law ($J(E) \sim E^2$). This result is shown in Fig. 3 for $T = 3.1$ K. At T related to the range at which the NDR occurs, the linear initial part of $J(E)$ characteristic is very small and changes to the Child-Langmuir law. This result is presented in Fig. 4 for $T = 1.9$ K. Faster growth of current with increasing electric field as compared to the Mott-Gurney law can be explained by the beginning of the breakdown effects. The Child-

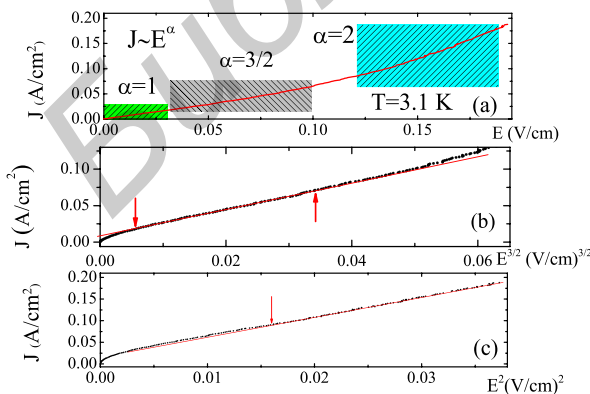


FIG. 3. (a) $J(E)$ curve at $T = 3.1$ K and $H = 0$. Shaded areas indicate E intervals in which one or another exponent α in the relation $J \sim E^\alpha$ is valid. (b) $J(E^{3/2})$ dependence at $T = 3.1$ K and $H = 0$. Arrows indicate the interval in the electric field in which the exponent $\alpha = 3/2$. (c) $J(E^2)$ dependence at $T = 3.1$ K and $H = 0$. The arrow indicates the electric field value above which the exponent $\alpha = 2$.

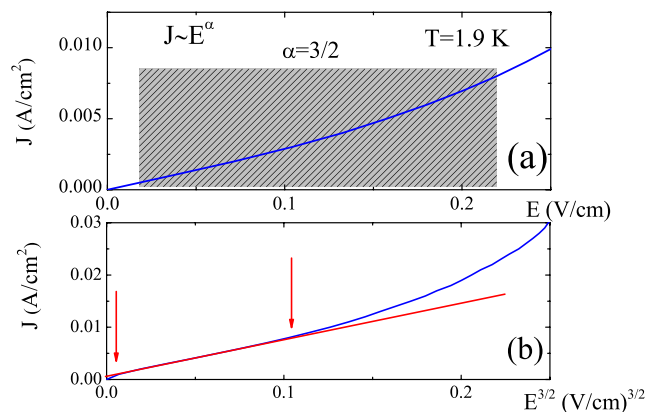


FIG. 4. (a) $J(E)$ curve at $T = 1.9$ K and $H = 0$. Shaded area indicates the E interval in which the exponent $\alpha = 3/2$. (b) $J(E^{3/2})$ dependence at $T = 1.9$ K and $H = 0$. Arrows indicate the interval in the electric field in which the exponent $\alpha = 3/2$.

Langmuir like behavior of $J(E)$ characteristics indicates the presence of charge accumulation, which is important for the explanation of the NDR mechanism.

The obtained regions with NDR are similar, at first glance, to those caused by the impurity breakdown.¹¹ Nevertheless, we may exclude this possibility from the consideration. Indeed, the impurity breakdown is caused by the avalanche multiplication of carriers in the conduction band due to the impact ionization of neutral donors. The required electrical field in this case exceeds 100 V/cm,⁴ which is 2 orders of magnitude greater than our E_{th} .

From our point of view, the most plausible explanation for the NDR manifestation at low T and E consists in the process of the D^- states delocalization in the upper Hubbard band (UHB). The emergence of the delocalization in the UHB of a semiconductor at a certain critical concentration of impurities is known for a long time.¹² It was demonstrated that the delocalization could occur at N_d values much lower than the concentration of the MIT (N_M), at $N_d \approx 0.015N_M$.¹³ For Sb doped silicon $N_M = 3 \times 10^{18} \text{ cm}^{-3}$,⁹ which is 3 times greater than in our samples, and so they are in the region of possible delocalization. The delocalization can also be reached by changing T and/or the degree of filling of the UHB, which is realized by the injection of the electrons. In our case, the impurity concentration is fixed and the delocalization could occur only due to the increase in the electron injection. At low degree of the injection, the conductivity is low and is determined by the activation mechanism. Thus, it is necessary to consider the degree of filling of the neutral D^0 states by electrons.

The appearance of the NDR usually is associated with the presence of a positive feedback.⁴ In the considered case, from a macroscopic point of view, the NDR may be caused primarily by such processes as charge accumulation and discharge in Si, which is controlled by the presence of a positive feedback. This can be explained as follows. At the initial low conductivity part of $J(E)$ curve, the magnitude of the current is low and slightly increases until the electric field reaches a threshold E_{th} . When $E < E_{th}$, the magnitude of J does not exceed 50 mA/cm² at $H = 0$ and $T = 1.9\text{--}2.5$ K (see Fig. 1(a)). As we demonstrated, in the T range 2.4–4.1 K, the conductivity is of the simple activation type (inset to Fig. 1(a)). In this case, at small degree of compensation, at the beginning of the electron injection, the neutral D^0 states will be filled by electrons and the space negative charge in Si will be accumulated. Thus, the D^- states are formed. The accumulated space charge will restrict and monitor the current flow. This is confirmed by the fact that the $J(E)$ dependence is described by the Child-Langmuir law (see Fig. 4). When a certain concentration of D^- states is achieved (at $E = E_{th}$), there is a change in the charge state. Obviously, the local electric field E_l , which acts on the D^- states, differs significantly from E_{th} . Indeed, the sufficient negative charge of the critical D^- states concentration creates a substantial E_l that can ionize D^0 states (see below). As a result, new D^+ states arise in the sample.¹² The appearance of sufficiently large local electric fields ensures that the two adjacent neutral tunnel-related donors will be transferred to the charge state: $D^0 + D^0 \rightarrow D^+ + D^-$, as it occurs when the substantial local electric field is applied in nanostructures to individual donors.^{14,15} In addition, under the

action of the local electric field, the energy of D^- states decreases and bounded excited states D^{-*} could be formed.¹⁶

The appearance of large E_l accelerates the process of delocalization due to the decrease in the binding energy of the D^- states and the formation of the D^{-*} states. These processes are characterized by the presence of a positive feedback, which causes the increase in the concentration of the D^- states and acceleration of their delocalization due to the electron-electron interactions on the D^- states. The presence of this positive feedback is a key process in the emergence of the observed NDR.

Let us find the confirmation of the above qualitative reasoning by evaluating the magnitude of the local electric field that is needed to compensate the activation energy $\epsilon \approx 17$ K. In our case, the electric field is created by the local field of neighboring electrons located at D^- states, E_l , which can be expressed as

$$E_l = \frac{1}{4\pi\epsilon_0\epsilon_s r_s^2} \sum_{i=1}^n \frac{q\mathbf{r}_i}{|\mathbf{r}_i|^3}, \quad (1)$$

where ϵ_0 is the permittivity of vacuum, ϵ_s is the permittivity of Si, q is the elementary charge, $r_s = (3/4\pi N_{D^-})^{1/3}$ is the average distance between electrons located at the D^- states, N_{D^-} is their concentration, \mathbf{r}_i is the normalized to the r_s value the radius-vector of the i -th electron at the point at which the electric field is determined and n is a number of neighboring electrons for which the sum is taken ($n = 8$). The only unknown variable in Eq. (1) is N_{D^-} . To estimate this quantity, it should be noted that the E_l value influences the ionization of D^- centers. When all of them are delocalized, it means that the E_l value could be associated with the delocalization field, E_l^{deloc} . The probability of the delocalization of the D^- centers, in turn, can be estimated within the model of ionization of a negatively charged center that takes into account a contribution of the electron-phonon interaction¹⁷

$$P(\epsilon) \sim \exp\left(-\frac{\epsilon}{k_B T} - \frac{2\epsilon\tau_1}{\hbar} + \frac{\sqrt{2m^*}\epsilon^{3/2}}{E_l q \hbar}\right), \quad (2)$$

where m^* is the effective mass of electron, \hbar is the reduced Planck's constant, k_B is the Boltzmann constant, and τ_1 is the characteristic time of the transition from D^- to D^0 state. The quantity $\hbar/2\tau_1$ is of the order of the phonon energy $\epsilon_{ph} \approx 15\text{--}65$ meV for the case of weak electron-phonon interaction, which is characteristic of Si. The delocalization of all D^- centers occurs when the exponent term in Eq. (2) is equal to 1. In this case, the E_l should be substituted by E_l^{deloc} . Substituting the obtained from Eq. (2) $E_l^{deloc} \approx 7 \times 10^3$ V/cm into Eq. (1) instead of E_l , we extract the concentration of D^- centers, which corresponds to E_l^{deloc} , $N_{D^-}^{deloc} \approx 6 \times 10^{16} \text{ cm}^{-3} \ll N_d$. Therefore, the local electric field could compensate the activation energy ϵ .

Influence of the magnetic field fits well with the picture of the phenomenon described. Indeed, the external magnetic field counteracts the achievement of the critical concentration of the D^- states, at which the delocalization begins. Both the Lorentz force, which reduces the coefficient of capture of injected electrons to the D^0 states, and the effect of

magnetic field on the spin-dependent electron transfer processes between D^0 states can cause this impact. In addition, the contribution of the Zeeman splitting of the impurity spin levels to the electronic transitions is also possible.^{15,18} Thus, to achieve a critical concentration of electrons in the UHB in the magnetic field required, it is necessary to increase the level of the electron injection, which leads to an increase in the E_{th} . On the other hand, the magnetic field reduces the electron binding energy on the D^- states. These two points further result, to our opinion, in the fact that a greater average rate of injection is required and the region with the NDR expands. The latter is because after the breakdown the contribution of the spin-dependent processes decreases with the change of the conduction mechanism. The magnetic field tends to align spins parallel, which reduces the speed of their capture on the D^0 states and weakens the localization of the D^- states. Finally, the difficulty in the delocalization in the presence of a magnetic field causes a substantial increase in the MR. In the inset of Fig. 2(b), we present the temperature dependence of the MR at $H = 80$ kOe. It is seen that at temperatures where the NDR effect is not observed, the MR becomes significantly lower.

Finally, we would like to discuss briefly how it is possible to engineer the proposed mechanism of NDR to realize it at higher temperatures. The observed low temperature NDR in Si occurs mainly due to the electronic states in the UHB. The activation energy ϵ is of the order of 17 K. Therefore, it is possible to increase the working temperature up to ≈ 15 K. This requires the suppression of the Mott hopping mechanism that involves D^+ states at $T > 4$ K, where it appears along with the transfer of the electrons over the D^0 and D^- states.⁸ Hopping suppression can be achieved by increasing the level of electron injection. This could be realized in the field effect transistor with the length of the Si channel less than 100 nm. The increase in the level of injection will allow to increase the concentration of nonequilibrium electrons, which will neutralize the emerging D^+ states and ensure the prevailing electron transfer over the D^0 states. To improve the homogeneity of the distribution of nonequilibrium electrons, the gradient of the electric and magnetic fields, created by the gate electrode fabricated, e.g., from Dy, can be used. The crucial role of the D^0 and D^- states in the electron transport in such nanostructures at $T = 4.2$ – 15 K has been experimentally proved in Refs. 16 and 18–21.

In summary, we demonstrated that the charge accumulation in noncompensated silicon could generate the delocalization of the induced D^- states in the UHB. This leads to the NDR effect on the CVC at low T and E . The microscopic mechanisms of electron capture at neutral centers, their

moving on them, as well as the delocalization of the D^- states are likely to be associated with such quantum-mechanical effects and processes as the Coulomb blockade and accompanying cotunneling, spin blockade, spin-dependent and dissipative tunneling, the electron-phonon interaction and other similar phenomena. Their manifestation in the NDR is still to be clarified. The observed effect is promising for electronic devices compatible with a widespread Si technology. Particular perspective could be such applications as high sensitive low temperature infrared detectors as well as detectors and generators of the THz radiation.

¹G. J. Ferreira, M. N. Leuenberger, D. Loss, and J. C. Egues, *Phys. Rev. B* **84**, 125453 (2011).

²C. H. Lee, X. Zhang, and B. Guan, *Sci. Rep.* **5**, 18008 (2015).

³F. Zu, Z. Liu, K. Yao, G. Gao, H. Fu, S. Zhu, Y. Ni, and L. Peng, *Sci. Rep.* **4**, 4838 (2014).

⁴*Negative Differential Resistance and Instabilities in 2-D Semiconductors*, NATO Science Series B: Physics, edited by N. Balkan, B. K. Ridley, and A. J. Vickers (Springer, 1993), p. 307.

⁵J. A. Berashevich, A. L. Danilyuk, A. N. Kholod, and V. E. Borisenko, *Mater. Sci. Eng. B* **101**, 111 (2003).

⁶N. Shukla, A. V. Thathachary, A. Agrawal, H. Paik, A. Aziz, D. G. Schlom, S. K. Gupta, R. Engel-Herbert, and S. Datta, *Nat. Commun.* **6**, 7812 (2015).

⁷D. Li, J. Shao, L. Tang, C. Edmunds, G. Gardner, M. J. Manfra, and O. Malis, *Semicond. Sci. Technol.* **28**, 074024 (2013).

⁸A. Fedotov, S. Prischeva, A. Danilyuk, I. Svito, and P. Zukowski, *Acta Phys. Pol. A* **125**, 1271 (2014).

⁹A. Ferreira da Silva, *Phys. Rev. B* **37**, 4799 (1988).

¹⁰P. Norton, *Phys. Rev. Lett.* **37**, 164 (1976).

¹¹R. E. Kunz, E. Schöll, R. Nürnberg, and H. Gajewski, *Solid State Electron.* **39**, 1155 (1996).

¹²E. Gershenzon, A. Mel'nikov, R. Rabinovich, and N. Serebryakova, *Phys. Usp.* **23**, 684 (1980).

¹³V. F. Bannaya, E. M. Gershenzon, A. P. Mel'nikov, R. I. Rabinovich, and I. E. Trofimov, *Zh. Eksp. Teor. Fiz.* **85**, 746 (1983) [*Sov. Phys. JETP* **58**, 434 (1983)].

¹⁴A. Fang, Y. C. Chang, and J. R. Tucker, *Phys. Rev. B* **66**, 155331 (2002).

¹⁵B. Weber, Y. H. Matthias Tan, S. Mahapatra, T. F. Watson, H. Ryu, R. Rahman, L. C. L. Hollenberg, G. Klimeck, and M. Y. Simmons, *Nat. Nanotechnol.* **9**, 430 (2014).

¹⁶R. Rahman, G. P. Lansbergen, J. Verduijn, G. C. Tettamanzi, S. H. Park, N. Collaert, S. Biesemans, G. Klimeck, L. C. L. Hollenberg, and S. Rogge, *Phys. Rev. B* **84**, 115428 (2011).

¹⁷V. N. Abakumov, V. I. Perel, and I. N. Yassievich, *Nonradiative Recombination in Semiconductors*, Modern Problems in Condensed Matter Sciences, Vol. 33, edited by V. M. Agranovich and A. A. Maradudin (North Holland, Amsterdam, 1991).

¹⁸H. Sellier, G. P. Lansbergen, J. Caro, S. Rogge, N. Collaert, I. Ferain, M. Jurczak, and S. Biesemans, *Phys. Rev. Lett.* **97**, 206805 (2006).

¹⁹E. Hamid, D. Moraru, J. C. Tarido, S. Miki, T. Mizuno, and M. Tabe, *Appl. Phys. Lett.* **97**, 262101 (2010).

²⁰G. Leti, E. Prati, M. Belli, G. Petretto, M. Fanciulli, M. Vinet, R. Wacquez, and M. Sanquer, *Appl. Phys. Lett.* **99**, 242102 (2011).

²¹A. Samanta, D. Moraru, T. Mizuno, and M. Tabe, *Sci. Rep.* **5**, 17377 (2015).